PHYSICAL REVIEW A VOLUME 23, NUMBER 2 FEBRUARY 1981

Charge transfer of HCl^+ in Xe

R. H. Neynaber
Department of Physics, University of California, San Diego, La Jolla, California 92093 and La Jolla Institute, La Jolla, California 92038

S. Y. Tang
La Jolla Institute, La Jolla, California 92038

(Received 19 August 1980)

Absolute and relative cross sections Q were obtained for the charge-transfer reaction $HCl^+ + Xe \rightarrow HCl + Xe^+$. The reactants and products are in their ground electronic states, but HCl^+ and HCl may be vibrationally and rotationally excited. The studies were made by a merging-beams technique for a relative kinetic energy W of the reactants from nominally 0.01 to 870 eV. Relative Q and laboratory-energy distributions of Xe^+ indicate that (a) near-resonant charge transfer preceded by a capture, or orbiting, collision occurs for $0.01 \lesssim W \lesssim 0.6$ eV, (b) near-resonant charge transfer without capture occurs for $0.6 \lesssim W \lesssim 200$ eV, and (c) nonresonant charge transfer is dominant for $W \gtrsim 400$ eV. The near-resonant charge transfer is apprarently fostered by the matching of electronic-vibrational-rotational energy levels of the entrance and exit channels. This results in the conversion of internal energy of HCl^+ into internal energy of HCl.

INTRODUCTION

The efficiency of rare-gas halide excimer lasing action in a mixture of HCl and Xe is affected by various reactions occurring in the mixture. The determination at thermal energy of cross sections for these processes is, therefore, desirable. One such reaction is

$$HCl^+(X^2\Pi, v \geq 0) + Xe(^1S_0) \rightarrow HCl(X^1\Sigma^+, v \geq 0) + Xe^+(^2P_{3/2}), \quad (1)$$

which is 0.61 eV exothermic for the ground-vibrational level (i.e., $v = 0$) of HCl and HCl^+. If $Xe^+(^2P_{1/2})$ replaces $Xe^+(^2P_{3/2})$, the reaction will be endothermic by 0.70 eV. Later we will show that the most likely production is $Xe^+(^2P_{3/2})$ below relative energies of, perhaps 200 eV or so, although at higher energies $Xe^+(^2P_{1/2})$ may be important.

We have used a merging-beams technique to measure the cross sections Q and investigate the collision dynamics of reaction (1) over the nominal energy range $0.01 \leq W \leq 870$ eV (where W is the nominal interaction energy, or relative kinetic energy of the reactants). In addition to its importance to lasers, this effort is also of fundamental interest since so few experimental investigations have been made of asymmetric charge-transfer reactions over such a wide range of collision energy. Reactions involving ion-atom interchange and the same reactants as in reaction (1) are expected to be endothermic by several electron volts. This will prevent them from significantly competing with charge transfer even at the high end of our W range of investigation.

Our studies were made by measuring the total product Xe^+ current and laboratory-energy distributions of Xe^+. Laboratory energies of different species outside the interaction region will be designated by E with an appropriate subscript. For example, the lab energy of the incident HCl^+ will be E_{HCl^+}. Similarly, the energy of the incident Xe will be E_{Xe}, but also is labeled E_2 since, as shown below, it is generated from source 2.

EXPERIMENTAL

A schematic of the merginig-beams apparatus is shown in Fig. 1. The general technique for obtaining data and the procedure for extracting Q from lab-energy distributions have been discussed.[1(a),1(b)] With the aid of the schematic mentioned above a brief description of the experiment will be given. Ions of H^1Cl^{35} were generated from HCl gas in the electron-impact source 1 and, after mass analysis in the merging magnet, passed into the interaction region. The energy of the ionizing electrons E_e in this source was usually about 60 eV. The charge-transfer cell, after the merging magnet, was not used in this experiment. Xenon ions were generated in the electron-impact source 2. After mass analysis in the analyzing magnet, the Xe^+ passed into a charge-transfer cell containing Xe gas. The E_e in source 2 was about 21 eV, which is below the threshold for production of the lowest-lying metastable state of Xe^+. This assured that only ground state Xe^+ reached the charge-transfer cell. Some of the Xe^+ entering the cell was converted to neutral Xe in the cell by resonant charge transfer. The remainder of the Xe^+ was collected on the condenser plates following the cell. The xenon neutral beam from the cell then merged with the HCl^+ beam from source 1 in the merging magnet, and finally, both beams

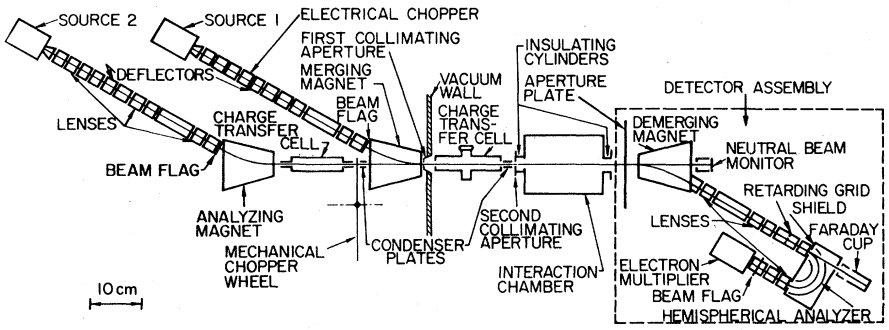

FIG. 1. Schematic of merging-beams apparatus. Apertures are not to the scale shown.

entered the interaction region where Xe^+ was generated by reaction (1). The Xe^+ was detected in the detector assembly, which consisted, among other components, of a retarding grid to eliminate undesired Xe^+ (principally from reactant Xe stripped in the residual gas), a 180° spherical electrostatic condenser (that acted as an energy analyzer), and a Johnston MM-1 electron multiplier. Chopping of beams 1 and 2 at 330 and 230 Hz, respectively, resulted in a modulated output of the multiplier of 100 Hz, which was fed into a lock-in amplifier followed by a recording system.

A potential P was applied to the interaction region so that Xe^+ formed inside this region would, upon leaving it, have a different energy than Xe^+ formed outside. The detector assembly could then be set to accept only Xe^+ formed inside. If E_{Xe^+} is the energy of Xe^+ outside the region, then $E_{Xe^+} - P$ is the energy inside. Similarly, the energy of the incident HCl^+ inside is $E_{HCl^+} - P$. The energy of the incident Xe is the same inside and outside and, as mentioned previously, is E_{Xe}. For a given range of W, E_{HCl^+} was fixed and E_{Xe} was varied. For example, for $0.01 \leq W \leq 10$ eV, $E_{HCl^+} = 1800$ eV while E_{Xe} was in the range 4700 to 5800 eV. The pressure in the interaction region, which was surrounded by a stainless steel can pumped by Ti sublimation, was approximately 4×10^{-9} torr.

BEAM COMPOSITION

The use of Xe in the first charge-transfer cell allowed a resonant charge-transfer reaction to occur in which ground state Xe^+ from source 2 was converted to a virtually pure beam of ground state Xe. The only other states of Xe which could be left in the beam at the interaction region are the $^3P_{2,0}$ metastable states and high-lying Rydberg states. These metastables have energy levels which would result in endothermicities for their production by charge transfer in the range 8–10 eV. The adiabatic criterion for asymmetric charge transfer indicates that the cross-section curves for their production would peak at energies E_P greater than 1 MeV.[2] The magnitude of the peak Q for such curves is close to the cross section for the resonant charge transfer of the incident ion at E_P, and the Q fall off rapidly at energies below the maximum.[3] This means that the Q for metastable production at E_{Xe} in our experiment (i.e., several thousand eV) will be small compared to the Q for the production of ground state Xe by resonant charge transfer since the latter Q increase with decreasing W.

The situation for the production of Rydbergs is similar. The endothermicities are even larger in this case, however, and the resultant Q would be smaller than that for the metastables. In addition, the electric field across the condenser plates following the cell containing Xe will tend to quench any Rydbergs.

The stable isotopes of Xe range from 124 to 136 amu. We estimate that five of these isotopes (between 129 and 134 amu) passed through the analyzing magnet and the charge-transfer cell and contributed to measured signals. The effect of these isotopes on the actual W and Q for reaction (1) will be discussed later.

There are two attractive electronic states of HCl^+; The $X^2\Pi$ ground state (at 12.74 eV above the ground state of HCl), and 3.55 eV above this, the $A^2\Sigma^+$ first excited state. Since the $A^2\Sigma^+$ state can make allowed transitions to the $X^2\Pi$ state during the transit time of HCl^+ from source 1 to the interaction region, it is assumed that the HCl^+ in the interaction region was in the ground electronic state. However, various vibrational and rotational states could be excited, and the population of these states is unknown. In the future we will refer to just the vibrational population with the understanding that rotational excitation also exists.

Potential curves and constants indicate that the equilibrium distance r_e for the $X^2\Pi$ state of HCl^+

is only about 3% larger than that for the $X^1\Sigma^+$ state (i.e., ground state) of HCl, but the r_e for the $A^2\Sigma^+$ state of HCl^+ is about 19% larger.[4] Because of these differences in r_e, the potential curves show that direct Franck-Condon transitions from HCl to HCl^+ induced by electron impact, such as in source 1, would be expected to result in little vibrational excitation of the $X^2\Pi$ state of HCl^+ but considerable vibrational excitation of the $A^2\Sigma^+$ state. This excitation in the latter state can then be transferred to the $X^2\Pi$ state by allowed electronic-vibrational transitions. Further modification of the vibrational population of the $X^2\Pi$ state could be expected to occur before the HCl^+ reaches the interaction region by infrared vibrational transitions within the state. The point is that the vibrational population of the $X^2\Pi$ state of HCl^+ presumably occurs in source 1 indirectly through transitions from the $A^2\Sigma^+$ state, which is populated directly by electron-impact ionization of HCl. The population of the $A^2\Sigma^+$ state would be determined by Franck-Condon factors, the Q curve for ionization by electron impact, and E_e in source 1. The threshold for this Q curve is $E_e \approx 16$ eV.

We made an attempt to determine the effect the vibrational population of the $X^2\Pi$ state of HCl^+ had on the measured Q for reaction (1). This consisted of varying E_e in source 1 and observing the measured, or effective, cross section Q_{eff}, which is defined as the composite Q for all the states of HCl^+ that existed in our experiment. The result for $W = 2.2$ eV is shown in Fig. 2. For $E_e \gtrsim 30$ eV it appears that the relative Q_{eff} is nearly constant at a value between 1.1 and 1.2. It is assumed that the scatter of data points about such a value is due to experimental error.

The Q_{eff} rises as E_e is decreased from about 30 to 20 eV. However, the increase tapers off below 20 eV. Assuming that vibrational excitation is larger for $E_e > 20$ eV than for $E_e < 20$ eV, we conclude that such larger excitation results in smaller Q_{eff}. It appears that a plateau may exist in Fig. 2 for $16 \lesssim E_e \lesssim 20$ eV. We will designate this range as the region of minimum excitation and the state of HCl^+ generated in this range as minimally excited. No data were obtained below $E_e = 16$ eV, and, therefore, the behavior for pure ground state HCl^+ (i.e., no electronic or vibrational excitation) was not examined. As mentioned previously, the customary E_e for source 1 was about 60 eV. Lower E_e were not used because of reduced intensity of the HCl^+ beam. At $W = 2.2$ eV absolute Q_{eff} at such an E_e would be only about 14% lower than the absolute Q_{eff} for the region of minimum excitation.

Curves like that of Fig. 2 were taken for other W between 0.01 and 10 eV with similar results. This indicates that the shapes of the Q vs W curves (i.e., relative cross-section curves) for relatively highly excited and minimally excited HCl^+ are very similar, or, perhaps, the Q for the more highly excited states are negligible. The latter possibility seems quite unlikely, although it is conceivable that the Q for some of the more highly excited states of HCl^+ are negligible and that the relative cross-section curves for the other highly excited states are like those for minimally excited HCl^+. As W increases above 10 eV, differences in the absolute Q_{eff} between highly and minimally excited HCl^+ are expected to be less. Data such as that in Fig. 2 but for $W > 10$ eV support this expectation.

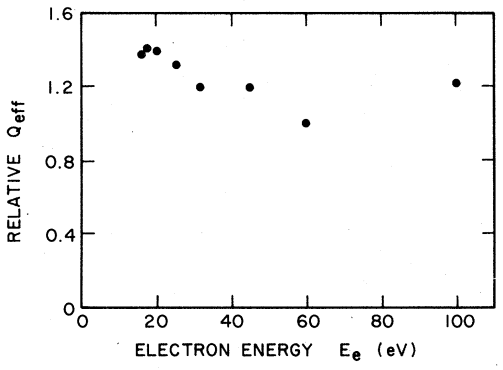

FIG. 2. Dependence of Q_{eff} on energy E_e of ionizing electrons in source of HCl^+ at $W = 2.2$ eV. Some electrons (relatively few) emitted from the ends of the ac heated filament have energies a few eV greater than E_e and some a few eV less than E_e.

RESULTS AND DISCUSSION

Relative cross sections

The measured relative Q for reaction (1) are shown in Fig. 3. Two important features should be noted: (a) Q decreases with increasing W for $W \lesssim 200$ eV, and (b) Q increases with increasing W for $W \gtrsim 400$ eV. The first feature is suggestive

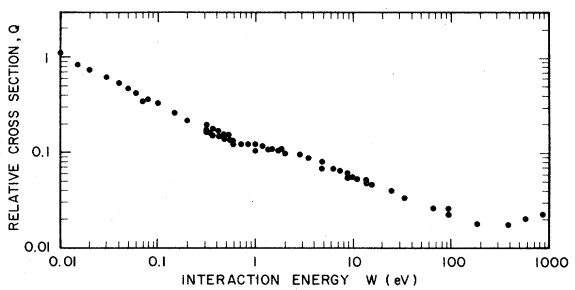

FIG. 3. Relative cross sections for $HCl^+ + Xe \rightarrow HCl + Xe^+$.

of a near-resonant process dominating the charge transfer and the second of a nonresonant process. In general, a nonresonant process could not explain the data for $1 \lesssim W \lesssim 200$ eV since the cross-section curve for such a process typically has the opposite slope in this energy range.

The dependence of Q on W for many resonant or near-resonant charge-transfer processes is $Q^{1/2} = A - B \ln W$, where A and B are constants.[5] To investigate further the near-resonant character of some of our data we have plotted our relative $Q^{1/2}$ versus $\ln W$ in Fig. 4. The straight line drawn between 0.6 and 200 eV appears to fit the data quite well in this range. Since the equation of this line is the same as the formula above, we conclude that a near-resonant process is taking place for $0.6 \lesssim W \lesssim 200$ eV. Since reaction (1) is quite exothermic when $v = 0$ for HCl and HCl^+, the near-resonant process between 0.6 and 200 eV occurs through the matching of electronic-vibrational energy levels of the entrance and exit channels. Such matching will leave the product HCl in excited vibrational levels.

An examination of the potential curves of $HCl(X^1\Sigma^+)$ and $HCl^+(X^2\Pi)$ shows that Franck-Condon transitions between such matching vibrational levels should be possible.[4] Such transitions, together with matching levels, are generally necessary for large cross sections for reactions such as (1). On the other hand, Franck-Condon transitions to matching levels will not be possible if $Xe^+(^2P_{3/2})$ in reaction (1) is replaced by $Xe^+(^2P_{1/2})$. On this basis we feel that the most likely state for the Xe^+ product, at least for $W \lesssim 200$ eV, is the $^2P_{3/2}$. It should be noted that cross sections for charge transfer of the $v = 0$ level of HCl^+ will be relatively small because transitions to v states of HCl cannot simultaneously be to matching levels and Frank-Condon-like.

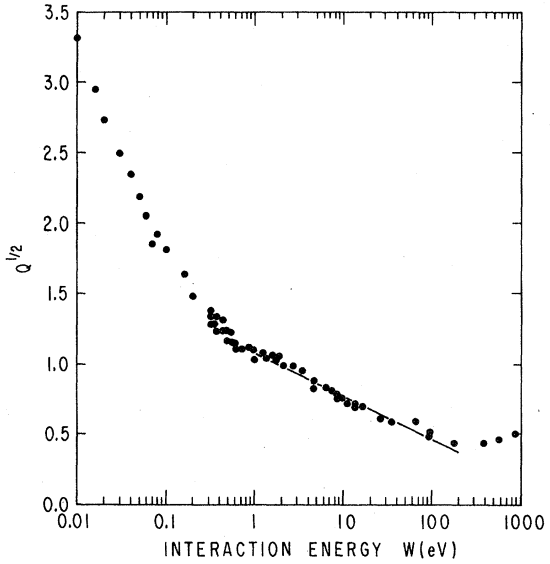

FIG. 4. Square root of relative cross sections as a function of W for $HCl^+ + Xe \rightarrow HCl + Xe^+$. The straight line was drawn as the best visual fit to the data between about 0.6 and 200 eV.

Another interesting observation in Fig. 3 is that $Q \propto W^{-0.51} \approx v^{-1}$ for $0.01 \lesssim W \lesssim 0.6$ eV, where v is the relative velocity of the reactants. This dependence is like that for the Langevin orbiting, or capture, model for ion-molecule collisions, which characteristically occurs at such low W.[6] In this model a complex is formed, which in general, can decay into various product channels. One of these channels can be charge transfer by electron tunneling. The charge transfer can be resonant or nonresonant. Later we will show that lab-energy distributions of the Xe^+ product indicate that a near-resonant process dominates. Wolf and Turner[7] have called such a process capture resonance. Presumably the near resonance is possible, as explained previously, through the matching of vibrational levels. There is a maximum impact parameter b_0 above which the Langevin model does not apply, and below which it does and a complex is formed. The Langevin cross section is thus πb_0^2, and, if charge transfer takes place after capture, the cross section can be expressed as $f\pi b_0^2$, where f is the fraction of captures resulting in charge transfer.[7] Wolf and Turner point out that if only electron transfer between an ion and a neutral occurs after capture, then the expected value of f is 0.5.[7] However, in our case as noted above, charge transfer of the $v = 0$ state of HCl^+ (and, perhaps, of relatively high v states) is not a significant channel after capture, and, hence, f would be less than 0.5.

At low W, generally less than an electron volt or so, b_0 is relatively large, and capture resonance dominates over simple charge transfer, or over what Wolf and Turner[7] call noncapture resonance. As W increases above an electron volt, b_0 decreases, and the impact parameter for noncapture resonance becomes larger than b_0. Then simple charge transfer becomes the main reaction channel. A theory for such noncapture resonance has been developed by Rapp and Francis.[3] In such processes the charge transfer takes place with little momentum transfer and rectilinear paths. This is quite different from capture resonance, which results in curved orbitals. In between the regions of capture resonance and noncapture resonance (i.e., for W between a few tenths and a few electron volts) there is a transition region in which the orbitals are also curved. Theoretical cross sections for this region have been

derived by Wolf and Turner.[7]

From the above discussion we identify the near-resonant process characterized by the straight line in Fig. 4 as noncapture resonance. It is seen in Figs. 3 and 4 that for W near 200 eV the Q for this noncapture resonance becomes relatively small. For higher W a new process begins to appear and dominates the charge transfer. As we have previously indicated, this process has the character of a nonresonant reaction with concomitant energy defects. Perhaps reaction (1) with ground-state reactants and products occurs, or $Xe^+(^2P_{1/2})$ is produced. Random errors in Fig. 3 are estimated to be ± 10%. In addition, transverse velocities[8] could increase our nominal, or quoted, W's by an energy W_T no greater than 0.02 eV. A $W_T = 0.02$ eV could result in reductions of the Q in Fig. 3 of 15, 9, 2, and 1% for nominal W's of 0.05, 0.1, 0.5, and 1 eV, respectively. Below $W = 0.05$ eV, the reductions would be more significant.

The measured signals S for $W \lesssim 0.6$ eV were virtually constant. It is highly unlikely that this result is an experimental artifact since many reactions have been studied with our merging-beams apparatus below $W \approx 1$ eV which do not give constant signals. These include Penning and associative ionization in the He*-He* [Ref. 9(a)] and Ne*-Ar* [Ref. 9(b)] systems, rearrangement ionization in collisions of H_2^+ with He [Ref. 9(c)] and of He* with H_2 [Ref. 1(a)], charge transfer of Ar^+ in Ar [Ref. 9(d)] and He^+ in Ne* [Ref. 9(e)], and ionization of Na in collisions of Na with O_2.[9(f)]

Thus, in the present experiment, since S is constant for $W \lesssim 0.6$ eV and $S \propto Q W^{0.5}$, then $Q \propto W^{-0.5}$, which is the result we have already quoted.[8] The existence of transverse velocities will not change the constancy of S. Therefore, even with transverse velocities there will still be a range of low W in which $Q \propto W^{-0.5}$ and in which the Langevin model applies.

As mentioned previously, the Xe beam consisted of several isotopes which contributed to our measured signals. For a given E_{Xe} and E_{HCl^+} each of these isotopes will correspond to a different relative collision energy. The W's quoted in this paper are nomial relative energies based on the abundance-weighted average of these Xe isotopes (i.e., 131.3 amu).

To assess the effect of these isotopes on our relative Q, we assumed a shape for a curve Q versus actual relative collision energy W_a. With this curve we calculated a curve of signal S versus W and compared this with our measured S-W curve. We iterated this process until we obtained an S-W curve which agreed with our measured curve. The Q-W_a curve which resulted in this agreement looks very much like that of Fig. 3. We conclude that Fig. 3 is a reasonably accurate graph of Q.

Energy distributions

Newton diagrams for reaction (1) are shown in Fig. 5. These are shown to help explain the measured laboratory-energy distributions of the product Xe^+. The diagrams are drawn for the case when the lab velocity of HCl^+, $|\vec{v}_{HCl^+}|$, is greater than the laboratory velocity of Xe, $|\vec{v}_{Xe}|$. In the "after-collision" diagram is shown a scattering sphere for Xe^+ in the center-of-mass (c.m.) system associated with a given W', where W' is the relative KE of the products.

Laboratory-energy distributions of Xe^+ are shown in Fig. 6. The energy of the Xe^+ outside the interaction region is shown with respect to $E_2 + P$, i.e., the energy scale of the distributions is $E_{Xe^+} - (E_2 + P)$. This difference is called ΔE. The data were taken in three steps. The first step results in points A designated as (○). These data were taken with HCl^+ faster than Xe and with the retarding grid several electron volts below $E_2 + P$ so as to allow Xe^+ from the desired reaction to pass through the 180° energy analyzer and to stop stripped reactant Xe. Points B are associated with the second step and are designated as (●). These points were originally taken with HCl^+ slower than Xe but transformed into points

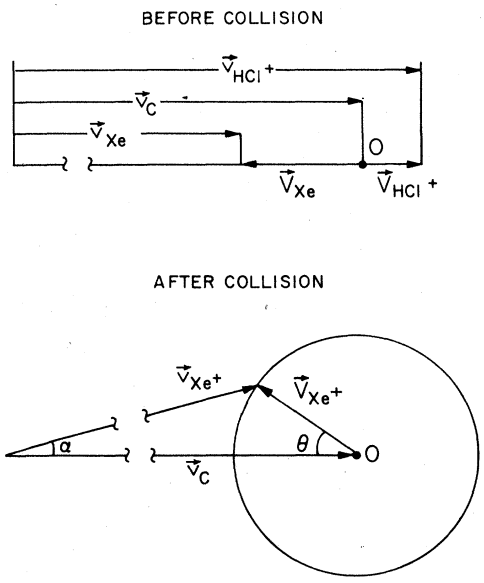

FIG. 5. Newton diagrams for $HCl^+ + Xe \rightarrow HCl + Xe^+$. Subscript c refers to the c.m., $\vec{v}$ is for laboratory velocity, and $\vec{V}$ is for velocity in the c.m. system. The scattering angle in the laboratory system is α; in the c.m. system it is θ. The drawing is not to scale. It should be noted that $|\vec{V}_{Xe^+}| \ll |\vec{v}_c|$.

for HCl^+ faster than Xe. This was accomplished by normalizing the intensity for a given point B to the same beam currents, detector gain, etc., as for the points A and assigning the point B a ΔE equal to the negative of its original value of $E_{Xe^+} - (E_2 + P)$. The two steps described above are necessary because of the stripping of reactant Xe in the residual gas. Detailed reasons for the procedure have been described previously.[10] The third step results in points labeled (□). These were obtained by adding the intensities of A and B taken with the potential of the retarding grid equal to the energy setting of the 180° energy analyzer so as to effectively block any Xe^+ with energy below that of the analyzer from passing through it.

The energy $E_2 + P$ is the energy the Xe^+ would have outside the interaction region if it underwent charge exchange with no momentum transfer. As shown by the Newton diagrams of Fig. 5, this would be the case when α and θ, the scattering angles in the laboratory and c.m. system, respectively, are zero (i.e., rectilinear paths are followed) and when the magnitude of the laboratory and c.m. velocities do not change with the collision. These conditions are associated with noncapture resonance. The energy ΔE is one measure of the deviation of the charge-exchange process from noncapture resonance. In Fig. 6 we will look for evidence of noncapture resonance and deviations from this. As discussed previously, such deviations should occur at both relatively high and low W.

A prototype of a distribution for noncapture resonance is shown at the top of Fig. 6. This is a distribution of a monoenergetic primary Xe^+ beam from source 2 at $E_2 = 4500$ and $P = 0$ and, as noted, is centered about $\Delta E = 0$. The spread in the distribution is due to the energy resolution of the detector, which is given by the full width at half-maximum (FWHM) divided by $E_2 + P$. This results in a value of approximately 1%.

It is noted in Fig. 6 that the main parts of the distributions at $W = 2$ and 7.5 eV are very similar to the prototype and, thus, are consistent with noncapture resonance. (The energy at the center of each of these distributions is just slightly greater than $\Delta E = 0$. The reason for this will be given below.) As discussed previously, Fig. 4 also indicates that noncapture resonance is occuring at these W.

The tails at $\Delta E > 0$ for the distributions at $W = 2$ and 7.5 eV are due to scattering of Xe^+ on spheres associated with W'. The magnitude of W' with respect to W cannot be determined from the distributions although much of the scattering in these tails could be on spheres for which $W' = W$. For $W = 2$ eV, $\theta > 90°$ (i.e., backward scattering) for points whose ΔE are greater than that of the arrow, where the arrow is the energy of Xe^+ (relative to $E_2 + P$) if Xe^+ had the velocity of the c.m.

The tails at $\Delta E < 0$ are also due to scattering on spheres associated with W', and since this scattering is at energies less than that of the c.m. arrow, $\theta < 90°$ (i.e., forward scattering) for such scattering. Furthermore, it can be shown that $W' > W$ for these tails and, therefore, the charge transfer is exothermic. Much of this forward scattering, which incidentally, is only a very small fraction of the total scattering, could be due to reaction (1) with HCl and HCl^+ in the ground-vi-

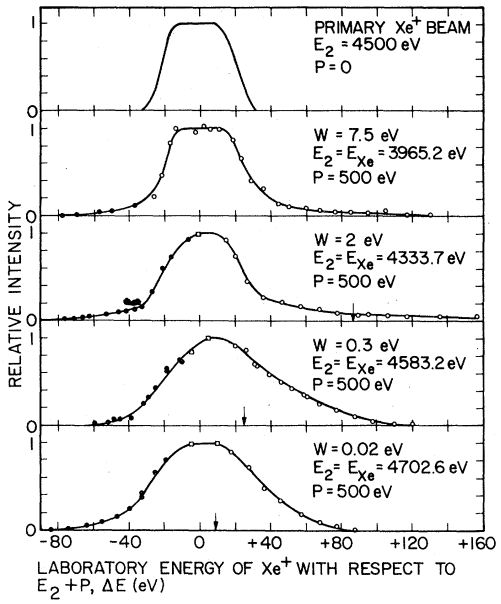

FIG. 6. Laboratory-energy distributions of Xe^+ production from $HCl^+ + Xe$ for HCl^+ faster than Xe. The energy scale of the distributions is ΔE, where $\Delta E = E_{Xe^+} - (E_2 + P)$. The distribution at the top of the figure is for a primary beam of Xe^+ at energy $E_2 = 4500$ eV and shows the resolution of the detector, whish is about $0.0095(E_2 + P)$. The energy of the Xe^+ product in the other distributions is $E_{Xe^+} - P$ inside the interaction region, where E_{Xe^+} is the energy of Xe^+ after it leaves the region, and P is the potential applied to the region. When Xe^+ leaves the interaction region it gains an energy equal to P. The energy of the reactant HCl^+ outside the interaction region is $E_{HCl^+} = 1800$ eV; inside the region it is $E_{HCl^+} - P$. The energy of Xe^+ if it had the velocity of the c.m. is designated by the arrow. At $W = 7.5$ eV, the arrow is off the figure at $\Delta E = 161.6$ eV. For $\theta = 0°$ and $W' = W$, $E_{Xe^+} = E_2 + P$, or $\Delta E = 0$. The following symbols have been used and are explained more fully in the text: (○), data points A taken with HCl^+ faster than Xe: (●), data points B originally taken with HCl^+ slower than Xe but transformed into points for HCl^+ faster than Xe; (□), data points taken by a method in which the intensities of A and B can be added to give the correct intensity. The smooth curves were drawn as the best visual fit to the data.

brational level since this would result in an exothermicity of 0.61 eV, as mentioned above.

At W = 2 and 7.5 eV the tails for $\Delta E > 0$ are somewhat larger than those for $\Delta E < 0$, and this tends to shift the energy at the center of each main distribution to a value slightly greater than $\Delta E = 0$. These tails, however, represent very little of the total scattering. As mentioned above, most of the scattering (i.e., the main distribution) is for noncapture resonance with $\theta = 0°$ and rectilinear paths. The tails are, for the most part, associated with nonrectilinear paths.

At the lowest W, viz., 0.02 eV, Langevin capture should occur as discussed previously. A complex will be formed and the resultant Xe^+ product will scatter isotropically. Such isotropic scattering should result in a distribution that is symmetric about the c.m. arrow. An examination of the distribution for $W = 0.02$ eV in Fig. 6 indicates that there is indeed a center of symmetry, unlike the other distributions in the figure for the Xe^+ product. However, this center is shifted just slightly from the c.m. arrow towards smaller energy. Either the shift is due to a small experimental error (such as an isotope of Xe resulting in a larger W and, thus, creating a tendency for noncapture resonance), or the Xe^+ product has some slight memory of its forward directed parent Xe. In any event, we think that the distribution largely reflects orbiting collisions.

The FWHM of the distribution at $W = 0.02$ eV is consistent with scattering in a sphere associated with $W' = 0.02$ eV. Thus, since $W' = W$, most all of the scattering at $W = 0.02$ eV can be described as due to capture resonance. If capture followed by nonresonance charge transfer prevailed at, for example, $W' - W = 0.61$ eV, which would be the case for reaction (1) with ground vibrational HCl and HCl^+, then the FWHM would be some 80 eV wider than that of the present distribution. The tails, or wings, of the present distribution do indicate some scattering in spheres such as this, but this scattering is only a minor contribution to the total charge transfer at $W = 0.02$ eV.

The distribution at $W = 0.3$ eV has no center of symmetry. Most of the scattering is at energies less than that of the c.m. arrow, and, hence, $\theta < 90°$ for such scattering. Thus, the Xe^+ has some memory of its Xe predecessor. In this sense the distribution reflects characteristics of noncapture resonance, but, since $\Delta E \neq 0$ for a large part of this forward scattering, there is an energy change between the Xe reactant and the Xe^+ product. Such behavior generally means that paths are not rectilinear, which is different from the case of noncapture resonance. In addition, the FWHM is larger than would be associated with noncapture resonance (i.e., larger than 1%). Finally, there is a rather large tail at ΔE greater than that of the c.m. arrow indicating significant scattering at $\theta > 90°$. These latter characteristics are like those of capture resonance. It appears, then, that $W = 0.3$ eV is in the previously described transition region between the energy ranges of capture and noncapture resonance.

As mentioned above, Fig. 3 shows that nonresonant charge transfer is the dominant process for $W \gtrsim 400$ eV. In principle, such nonresonant behavior for scattering centered about $\theta = 0°$ will cause the energy at the center of the Xe^+ distribution to shift from $\Delta E = 0$ to some other ΔE associated with the value of $W' - W$. However, for a given $|W' - W|$, the magnitudes of such shifts decrease with increasing W and are only a fraction of an electron volt for $W \gtrsim 400$ eV and expected $|W' - W|$ of about 0.6 to 0.7 eV. We have verified this experimentally, and do not include such distributions in Fig. 6 because of their mundane character.

Absolute cross sections

An absolute cross section was measured for reaction (1) at $W = 0.3$ eV and $E_e \approx 60$ eV with the result that $Q(0.3) = (2.6 \pm 30\%) \times 10^{-15}$ cm^2. From this value and Fig. 3, absolute values can be determined at all W. For example, at $W = 0.03$ eV, $Q(0.03) = (8.4 \pm 32\%) \times 10^{-15}$ cm^2. An upper limit to Q at low W is given by the Langevin capture cross section πb_0^2, which, at $W = 0.03$ eV, is 19.6×10^{-15} cm^2. From this value and $Q(0.03)$ we obtain $f = 0.43 \pm 32\%$, where, as discussed previously, f is the fraction of captures resulting in charge transfer and is expected to be less than 0.5. The $Q(0.03)$ for the region of minimum excitation is about 9.8×10^{-15} cm^2, or 16% larger than the value quoted above (see the section on beam composition). This results in an $f = 0.5$ for this region, which suggests that the population of the $v = 0$ state of HCl^+ in our beam is relatively small.

SUMMARY

Relative Q for reaction (1) indicate that (a) capture resonance occurs for $0.01 \lesssim W \lesssim 0.6$ eV., (b) noncapture resonance occurs for $0.6 \lesssim W \lesssim 200$ eV, and (c) nonresonant charge transfer prevails for $W \gtrsim 400$ eV. The laboratory-energy distributions of Xe^+ for reaction (1) shed further light on the kinetics. These indicate that there is actually a transition region in W between a few tenths of an electron volt and 1 eV or so in which reaction (1) shows characteristics of both capture and noncapture resonance. Apparently near-resonant charge transfer is possible through the matching

of excited vibrational levels of the reactant HCl^+ and excited vibrational levels of the product HCl. Thus, reaction (1) converts internal energy of HCl^+ into internal energy of HCl.

As expected, the distributions for the W region of noncapture resonance are consistent with most of the scattering at $\theta = 0°$ although the tails indicate the existence of a little angular scattering. For W below that of the region of noncapture resonance the distributions show more evidence of angular scattering. In fact, the distribution at $W = 0.02$ eV suggests, as expected, that orbiting collisions resulting in nearly isotropic scattering are dominant. All of the distributions for $W < 7.5$ eV indicate minor contributions from nonresonant charge transfer. The absolute cross section at $W = 0.03$ eV was determined to be $Q(0.03) = (8.4 \pm 32\%) \times 10^{-15}$ cm^2. From this value and the Langevin cross section we obtain $f = 0.43$.

ACKNOWLEDGMENTS

This research was sponsored by the Air Force Office of Scientific Research (AFSC), U.S. Air Force under Grant No. AFOSR-80-0244 and by the Office of Naval Research.

[1] (a) R. H. Neynaber, G. D. Magnuson, and J. K. Layton, J. Chem. Phys. 57, 5128 (1972); (b) R. H. Neynaber, G. D. Magnuson, S. M. Trujillo, and B. F. Myers, Phys. Rev. A 5, 285 (1972).

[2] J. B. Hasted, *Physics of Atomic Collisions* (Butterworths, London, 1964), p. 421.

[3] D. Rapp and W. E. Francis, J. Chem. Phys. 37, 2631 (1962).

[4] (a) H. J. Lempka, T. R. Passmore, and W. C. Price, Proc. R. Soc. London Ser. A 304, 53 (1968); (b) J. Raferty and W. G. Richards, J. Phys. B 6, 1301 (1973); (c) K. P. Huber and G. Herzberg, *Molecular Spectra and Molecular Structure* (Van Nostrand Reinhold, New York, 1979), Vol. 4.

[5] See, for example, A. Dalgarno, Philos. Trans. R. Soc. London Ser. A 250, 426 (1958).

[6] See, for example, G. Gioumousis and D. P. Stevenson, J. Chem. Phys. 29, 294 (1958).

[7] F. A. Wolf and B. R. Turner, J. Chem. Phys. 48, 4226 (1968).

[8] S. M. Trujillo, R. H. Neynaber, and E. W. Rothe, Rev. Sci. Instrum. 37, 1655 (1966).

[9] (a) R. H. Neynaber, G. D. Magnuson, and S. Y. Tang, J. Chem. Phys. 68, 5112 (1978); (b) R. H. Neynaber and S. Y. Tang, *ibid.* 72, 6176 (1980); (c) R. H. Neynaber and G. D. Magnuson, *ibid.* 59, 825 (1973); (d) R. H. Neynaber, S. M. Trujillo, and E. W. Rothe, Phys. Rev. 157, 101 (1967); (e) S. Y. Tang and R. H. Neynaber, Phys. Rev. A 18, 1925 (1978); (f) R. H. Neynaber, B. F. Myers, and S. M. Trujillo, Phys. Rev. 180, 139 (1969).

[10] R. H. Neynaber and G. D. Magnuson, J. Chem. Phys. 67, 430 (1977).